Thin crystal development and applications for hard x-ray free-electron lasers

Taito Osaka[*a], Makina Yabashi[b], Yasuhisa Sano[a], Kensuke Tono[c], Yuichi Inubushi[b], Takahiro Sato[b,d], Kanade Ogawa[b], Satoshi Matsuyama[a,e], Tetsuya Ishikawa[b], Kazuto Yamauchi[a,e,f]
[a]Department of Precision Science and Technology, Graduate School of Engineering, Osaka University, 2-1 Yamada-oka, Suita, Osaka 565-0871, Japan; [b]RIKEN SPring-8 Center, 1-1-1 Kouto, Sayo-cho, Sayo-gun, Hyogo 679-5148, Japan; [c]Japan Synchrotron Radiation Institute (JASRI), 1-1-1 Kouto, Sayo-cho, Sayo-gun, Hyogo 679-5198, Japan; [d]Department of Chemistry, School of Science, The University of Tokyo, 7-3-1 Hongo, Bunkyo-ku, Tokyo 113-0033, Japan; [e]Japan Science and Technology Agency, CREST, 4-1-8 Honcho, Kawaguchi, Saitama 332-0012, Japan; [f]Research Center for Ultra-Precision Science and Technology, Graduate School of Engineering, Osaka University, 2-1 Yamada-oka, Suita, Osaka 565-0871, Japan

ABSTRACT

We have developed a new method to fabricate ultrathin silicon single crystals, which can be used as spectral beam splitters for the hard x-ray regime, based on a reactive dry etching process using plasma at atmospheric pressure. The high crystalline perfection of the crystals was verified by both topographic and high-resolution rocking curve measurements using coherent x-rays at the 1-km-long beamline, BL29XUL of SPring-8. The development of thin crystals enables the construction of a split-delay unit and the provision of a dedicated branch for photon diagnostics. By using a 20-μm-thick Si(111) crystal in the symmetric Bragg geometry as a component of a Si(111) double-crystal monochromator, an arrival-time monitor using a destructive manner has been upgraded to a non-destructive method at SPring-8 Angstrom Compact free-electron LAser. Using the splitting crystals in a helium atmosphere can prevent oxidation, which can introduce a lattice distortion.

Key words: SACLA, hard x-rays, FEL, beam splitter, thin crystal

1. INTRODUCTION

The recent success of x-ray free-electron lasers (XFELs) such as the Linac Coherent Light Source (LCLS)[1] in the USA and SPring-8 Angstrom Compact free-electron LAser (SACLA)[2] in Japan, which provide exceptionally intense, spatially coherent, and femtosecond x-ray pulses, have and will open new frontiers in atomic physics,[3,4] structural biology,[5,6] and nonlinear x-ray optics.[7] Particularly, one of the key features of XFEL light, an ultrafast pulse duration, enables investigation of ultrafast phenomena induced by optical or x-ray lasers with femtosecond time resolution. In optical pump-XFEL probe experiments, the time resolution is generally limited to 150–300 fs because of the arrival-time jitter with respect to an externally synchronized event.[8] Further, XFEL pump-XFEL probe experiments in the hard x-ray regime have been hardly reported. We present here the results of recent activities to implement pump-probe experiments at SACLA with a time resolution comparable to the pulse duration.

The development of beam splitters for the hard x-ray regime enables construction of a split-delay unit, which can provide two replica XFEL pulses with a time delay controlled with sub-femtosecond accuracy, and to provide a dedicated branch for photon diagnostics or another experiments. One of the candidates for the beam splitters is a thin single crystal in the symmetric Bragg geometry that can spectrally split an XFEL pulse into transmitted (refracted) and reflected pulses with a simple and small impact on the XFEL pulse profiles both spatially and temporally.[9] To accomplish the beam splitting with intense transmission, thicknesses of <20 μm for silicon crystal and <100 μm for diamond crystal are desired. The thickness variation in an illuminated area should be <200 nm to achieve a negligible wavefront distortion of the transmitted pulses. So far, there are a few reports on thin silicon crystal[10, 11] because fabrication of the crystal with high

*Corresponding author: osaka@up.prec.eng.osaka-u.ac.jp; phone/fax +81 6 6879-7286.

Advances in X-Ray/EUV Optics and Components VIII, edited by Ali Khounsary, Shunji Goto, Christian Morawe, Proc. of SPIE Vol. 8848, 884804 · © 2013 SPIE
CCC code: 0277-786X/13/$18 · doi: 10.1117/12.2023465

crystalline perfection is extremely difficult. Further, lattice distortion can be induced by weak mechanical stress and affect the XFEL pulses.[11] A fabrication method that can produce thin crystals with any crystal orientation and a proffer of an effective method for preventing the lattice distortion are necessary in order to perform a wide range of time-resolved experiments and temporal photon diagnostics.

2. FABRICATION AND EVALUATION

2.1 Fabrication of ultrathin silicon crystals

Wet etching or chemical mechanical polishing (CMP) processes are typically used for thinning of silicon crystals. By the former method, the available crystal orientation is limited to that with low surface energy. By the latter, only a fully thinned crystal that possibly includes scratches can be obtained. The fully thinned crystal easily bends under mechanical stress and its own weight. Although near-perfect ultrathin Si single crystals supported by a thick Si frame across a SiO_2 layer have become available thanks to advancements in silicon-on-insulator technology, the difference in the coefficients of thermal expansion and the lattice constants between Si and SiO_2 has the potential to cause critical lattice strain for a high-order diffraction plane, for example, the (511) with a lattice spacing of less than 1 Å.

In the present work, a new technique to fabricate ultrathin all-silicon single crystals based on a reactive dry etching process using atmospheric-pressure plasma called plasma chemical vaporization machining (PCVM) has been developed.[12] In the PCVM process, the high-pressure atmosphere leads to generation of high-density reactive radicals and ions with low kinetic energies, which introduce little lattice damage to the work piece, resulting in localization of the plasma to a region where a high electric power is introduced. Si atoms on the surface of the work piece react with radicals, and then the products vaporize. By using fluoride gas as a component of the atmosphere for silicon crystals, it has been found that the removal rate scarcely depends on the crystal orientation owing to the high reactivity of the F radical. Although a removal rate from an area with crystal damage is higher than that from a perfect area, the finished surface is very smooth if the removal depth is deeper than 10 μm, e.g., the surface roughness is 0.1–0.2 nm root-mean-squared (rms) in a measurement area of 71 × 53 μm^2.

2.2 Topographic and high-resolution rocking curve measurements

To evaluate the quality of an ultrathin frame-shaped Si(511) crystal in the symmetric Bragg geometry fabricated using the PCVM technique schematically depicted in Fig. 1(a), topographic and high-resolution rocking curve measurements were performed at the 1-km-long beamline, BL29XUL[13] of SPring-8 in Japan. The x-ray beam from an undulator was reflected by a high-heat-load Si(111) double crystal monochromator (DCM). An energy resolution $\Delta E/E = 4.8 \times 10^{-6}$, where ΔE and E are the energy width and the central photon energy of reflected x-rays, respectively, which was smaller than the intrinsic Darwin width in the energy domain of the Si(511) diffraction of 8.3×10^{-6} was achieved by using a four-bounced Si(444) reflection arranged in the (−, +, +, −) geometry positioned in Experimental Hutch 1, 52 m downstream from the source. Further, an angular resolution better than 1 μrad was accomplished at Experimental Hutch 4 after the 1-km beam transport. The high-resolving x-ray probe was delivered to the Si(511) crystal at the Bragg angle $\theta_B = 45°$ for the (511) diffraction (E = 8.39 keV). The intensities of both the reflected and transmitted x-ray beams were measured by PIN photodiodes, and the reflection topograph was taken by a CCD camera unit with an effective pixel size of 6 × 6 μm^2. To avoid lattice bending by mechanical stress, the thin crystal was mounted on a holder without any stress to fix the crystal.

Figures 1(b), (c) and (d) show the topograph on the Bragg condition and the rocking curves, respectively. High contrast indicating crystal damage such as defects and scratches does not appear in the red rectangular area on the topograph corresponding to the thin area. Further, the rocking curve measured at any spot in the thin area agrees well with the calculated curve. Thicknesses of the pink and light green rectangular areas were evaluated to be 9.0 μm and 6.9 μm, respectively, which means the low contrast in the thin area shown in Fig. 1(b) is attributed to the thickness variation. These data indicate a sub-10-μm-thick all-silicon single crystal with high crystalline perfection can be obtained for any crystal orientation using the PCVM technique. Currently, we can provide ultrathin silicon crystals down to 4 μm with highly uniform thickness distribution in the thin area, although this (511) crystal includes a comparatively large thickness variation.

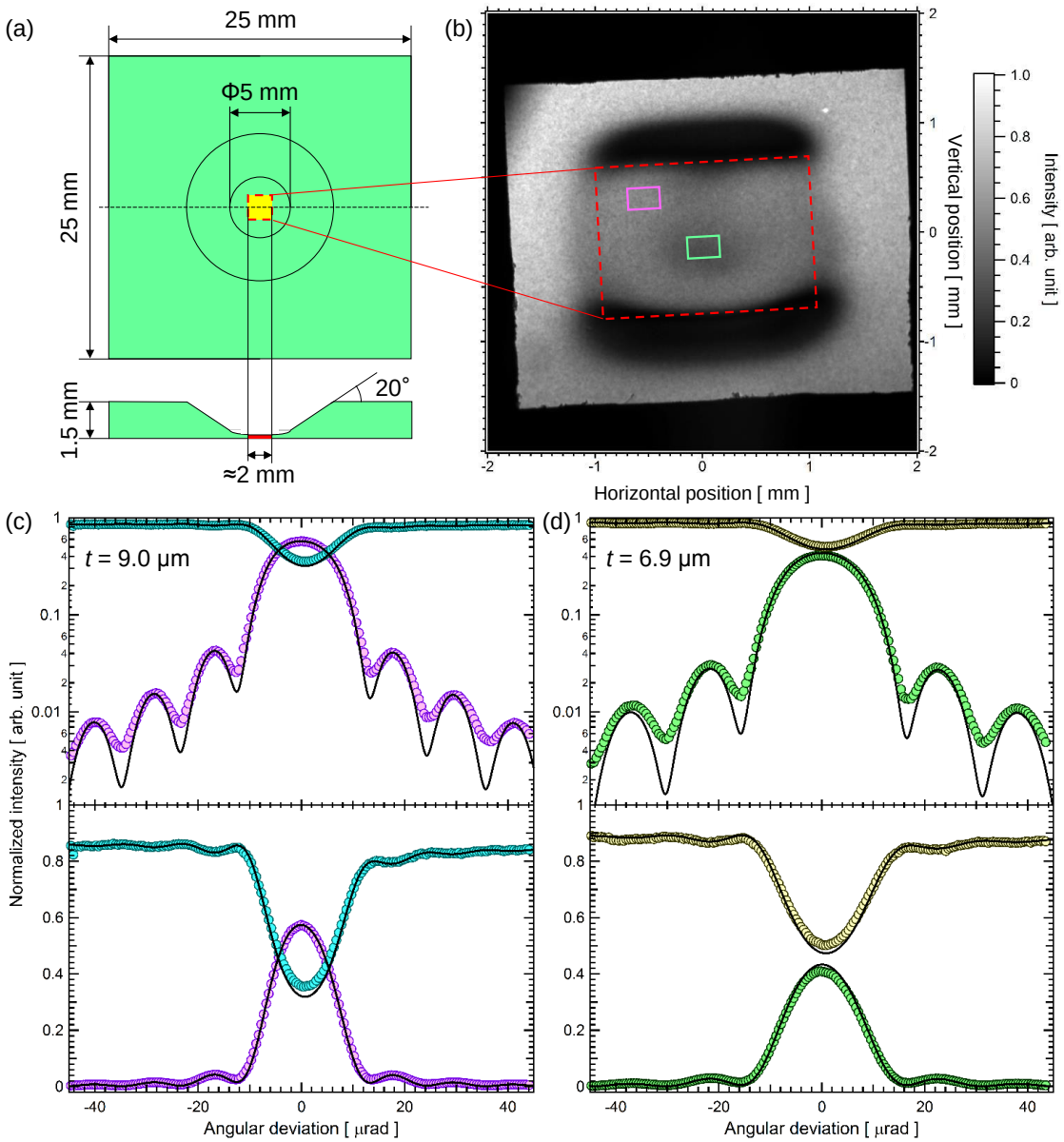

Figure 1 (a) Schematic of an ultrathin frame-shaped Si(511) crystal in the symmetric Bragg geometry; (b) reflection topograph on the Bragg angle for the (511) diffraction. Red dashed rectangular area corresponds to the thin area; (c) and (d) rocking curves measured at pink and light green rectangular areas on subpanel (b), respectively. Upper and lower curves are scaled logarithmically and linearly, respectively. Measured and calculated data are depicted as symbols and solid lines, respectively. The size of the x-ray probe was 0.3 × 0.2 mm^2.

3. APPLICATIONS OF ULTRATHIN SILICON CRYSTALS

3.1 Non-destructive arrival-time monitor

To measure the relative arrival-time jitter between the optical and XFEL pulses, several tools based on an XFEL pump-optical probe cross-correlation techniques have been developed.[14,15] However, some of them are based on destructive schemes. Here we present the work to upgrade the destructive arrival-time monitor to a non-destructive one using a thin Si(111) crystal.

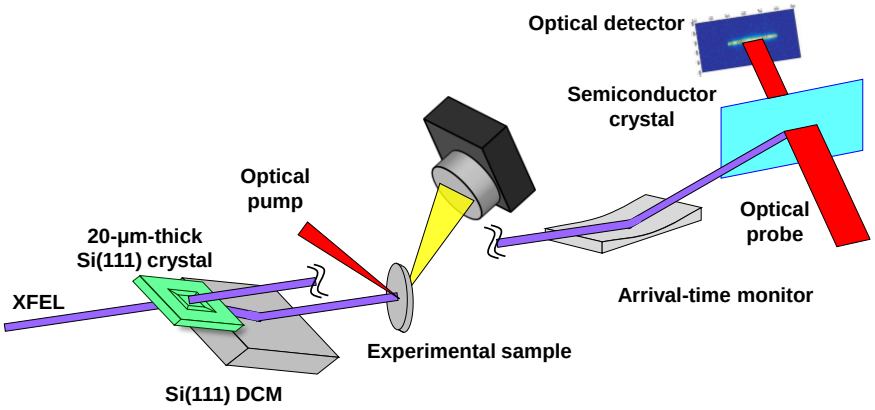

Figure 2. Schematic of a non-destructive arrival-time monitor system. An XFEL beam is split into a transmitted pink beam and a reflected monochromatic beam by the thin Si(111) crystal. The transmitted and reflected XFEL beams are simultaneously delivered to the destructive arrival-time monitor and an experimental sample, respectively.

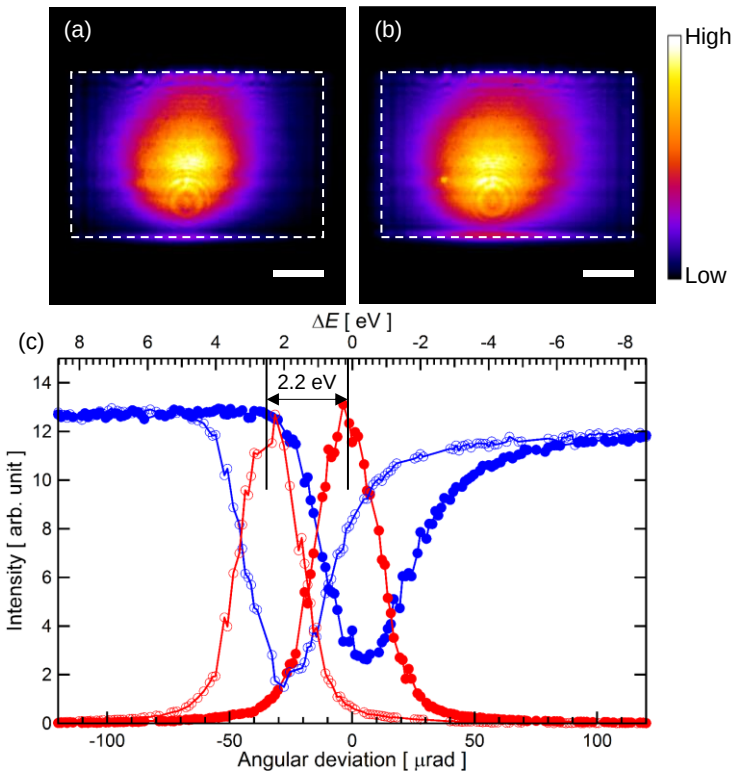

Figure 3. 100-shot-averaged (a) reflected and (b) transmitted 8.68-keV XFEL pulse profiles with scale bars of 0.2 mm. The dashed rectangular area corresponds to the slit size of 1.0 × 0.7 mm^2; (c) Measured rocking curves using a 12-keV XFEL beam with the permanently-installed Si(111) DCM. Unfilled symbols show the curve measured after 12 hour operation.

The proposed non-destructive arrival-time monitor system is depicted in Fig. 2. By using a beam splitter as a component of a Si(111) DCM, transmitted pink (upper branch) and reflected monochromatic (lower branch) XFEL beams can be provided. The transmitted and reflected XFEL beams are simultaneously delivered to the destructive arrival-time monitor and an experimental sample, respectively. Comparable flux to that used with the permanently-installed Si(111) DCM application is desired by user communities. To comply with these demands, a Si(111) crystal in the symmetric Bragg geometry with a thickness of 20 μm supported by a 500-μm-thick frame was applied as the beam splitter crystal, which is a component of the beam splitting Si(111) DCM as shown in Fig. 2. The crystal has the potential to provide a

transmitted XFEL pulse with a transmissivity higher than 10% corresponding to a pulse energy of >20 μJ for x-rays of 6–12 keV and a reflected pulse with an on-demand flux because the crystal can be assumed as a thick crystal for the Si(111) diffraction. The fabricated Si(111) beam splitter has a flat thin area of 3 × 5 mm^2 that is sufficiently wide for an XFEL beam. The high quality was verified with topographic and high-resolution rocking curve measurements similar to those explained in Chapter 2. At the LCLS, a large lattice distortion of thin silicon crystals induced by the impact of high-repetition-rate intense XFEL pulses has been found.[11] Therefore we evaluated the performance of the Si(111) beam splitter under XFEL irradiation at SACLA. XFEL pulses with full-power (0.2 mJ) and 10-Hz repetition rate operation mode were used. The reflected and transmitted 8.68 keV XFEL pulse profiles averaged over 100 shots are shown in Figs. 3(a) and (b), respectively. Similar profiles, meaning that lattice distortion did not occur, were obtained. Further, measurement of the arrival-time jitter can be achieved by means of the transmitted 12-keV XFEL pulses. Although a 2.2-eV energy drift was found during the first 12 h of operation as shown in Fig. 3(c), since then the central photon energy of the reflected XFEL beam has been stable. This non-destructive arrival-time monitor system has been installed and widely used for optical pump-XFEL probe experiments at BL3 of SACLA.

3.2 Split-delay unit

One of the valuable applications of the beam splitter is as a split-delay unit. An XFEL pulse is split into two replica pulses by the first beam splitter in a split-delay unit, then each pulse is transported to the second beam splitter and recombined onto the same axis with a time delay depending on the difference in the path lengths. The key feature of a split-delay unit is its jitter-free configuration, which has the potential to achieve sub-femtosecond time resolution if one of the path lengths is adjustable. For hard x-rays, a split-delay unit using wedge-shaped Si(511) crystals in the Laue geometry has been reported.[16] However, the transported flux of each pulse is 0.3% that of an input XFEL pulse with a Si(111) DCM application because of the narrow Darwin width of the Si(511) diffraction and the difference in the dispersion between the Laue and Bragg crystals. Although the flux becomes larger when using the Bragg crystal as the beam splitters, the available photon energy is limited to 8.39 keV because the scattering angle is fixed at near 90° to simplify the system. We proposed a split-delay unit with a high flux and a wide energy range applying the Si(220) diffraction in the Bragg geometry and a linear stage system moving along a variable direction. A 30-times-higher flux than that of the reported split-delay unit and an energy range of 7–12 keV will be ideally accomplished by the proposed unit.

To implement the construction of the split-delay unit, 3 ultrathin frame-shaped Si(220) crystals including a spare were prepared. The thicknesses of the crystals were evaluated to be 6.4–6.8, 7.7–8.0, and 8.3–8.5 μm by means of the high-resolution rocking curve measurement described in Chapter 2. Figure 4 shows their reflection topograph on the Bragg condition for the (220) diffraction measured at SPring-8 with a (+, −) parallel arrangement using 10-keV x-rays; the Bragg angle was 18.8° that is smaller than the taper angle of 20°. All of the topographs show uniform intensity distribution in the thin area. The available beam size along the vertical direction was evaluated to be larger than 0.3 mm that is equivalent to the FWHM of the SACLA XFEL beam at 100 m downstream from the end of the undulator. The measured peak reflectivity of >80% is a nearly ideal value. Therefore, the key component of the split-delay unit, beam splitter has been prepared.

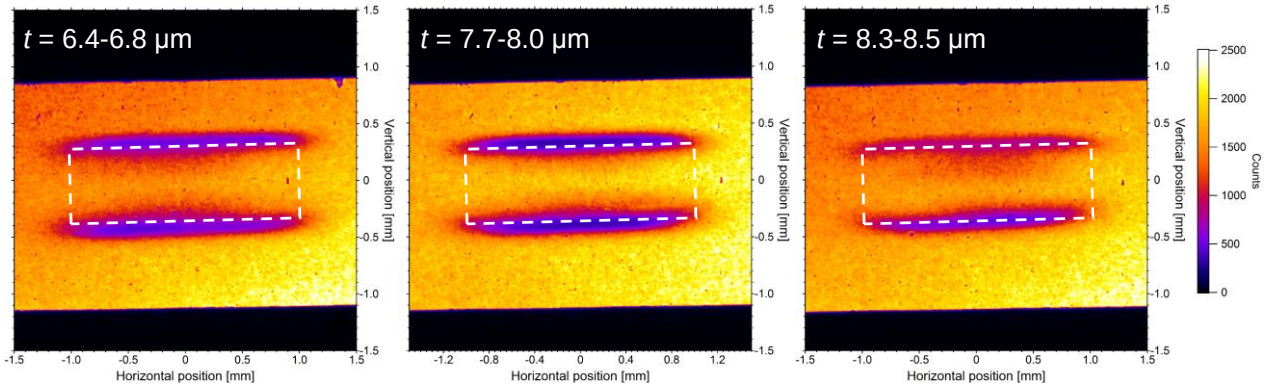

Figure 4. Reflection topographs of three ultrathin frame-shaped Si(220) crystals for the split-delay unit measured by using the (+, −) parallel arrangement with 10-keV x-rays. The Bragg angle was 18.8°. Dashed rectangular area corresponds to the thin area.

4. EFFECTIVE USE OF ULTRATHIN CRYSTALS

A wide effective splitting area is necessary for a wide range of applications of the beam splitter to realize stable use and high throughput. Although this is achievable by expanding the thin area, fabrication of a sub-10-μm-thick perfect crystal with a wide thin area is now a challenging issue because a wide ultrathin crystal is easily bent by various causes such as local thermal expansion and membrane stress. Further, a shift of the Bragg peak due to the refraction effect has been found around the edge of the thin area including a steep taper as shown in the topographs of Figs. 1(b) and 4. Time evolution of the "shadow" area has been also observed in operation under x-ray irradiation. Investigation of the cause and how to block this evolution is presented here.

To investigate the cause of the shadow evolution, reflection topographs for the Si(440) diffraction were sequentially measured under several conditions: 1) cooled with water in a helium atmosphere, 2) heated in a helium atmosphere, and 3) heated in ambient air. The experiment was performed at the 1-km-long beamline, BL29XUL of SPring-8 using a 16.325-keV x-ray probe and a (+, −) parallel arrangement with an analyzer crystal. The Bragg angle was 23.3°. The thin Si(220) crystal, which was the same as that shown in the left panel of Fig. 4, was cleaned by means of H_2SO_4 + H_2O_2 and 10% HF solutions before the measurements. Figure 5 shows the sequential line profiles of the topographs along a horizontal position 0 and the topographs at several operation times. Although large lattice distortion that was probably

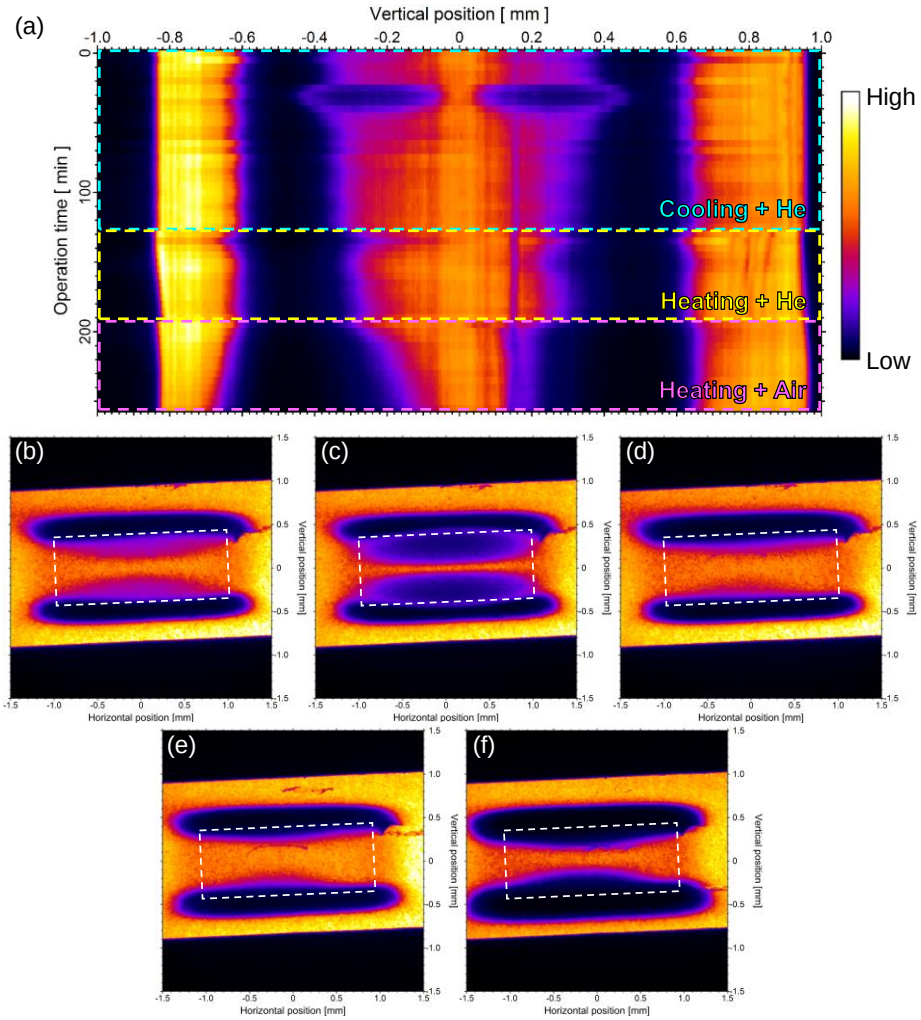

Figure 5. (a) Sequential view of the line profiles of the Si(440) reflection topographs on the Bragg condition at horizontal position 0 as a function of operation time. The Bragg angle is 23.3° for the 16.325-keV x-ray probe; (b–f) variation of the reflection topographs at operation times of (b) 0 min (cooled in helium atmosphere), (c) 30 min, (d) 125 min, (e) 190 min (heated in helium atmosphere for 60 min), and (f) 255 min (heated in ambient air for 60 min). Dashed rectangular area corresponds to the thin area of 2 × 2 mm^2.

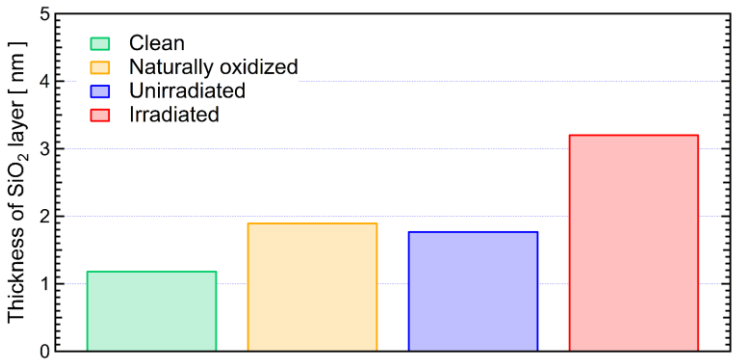

Figure 6. Thickness of the SiO_2 layer on the silicon surface under several conditions: clean (green), naturally oxidized (yellow), unirradiated (blue), and irradiated by x-ray photons (red). The thickness was measured by spectroscopic ellipsometry. The density of the SiO_2 layer was assumed to be the same as the thermal oxide.

originated by local thermal expansion was observed at an operation time of 25–40 min as shown in Figs. 5(a) and (c), the distortion rapidly disappeared, and the shadow area persisted during operation in the helium atmosphere. In ambient air, the shadow area gradually expanded. Therefore, the cause of the shadow evolution exists in ambient air.

It has been found that the shadow area returns to the initial state after cleaning the crystal. This fact indicates that some layer is grown on the crystal surface under x-ray irradiation. The thickness of the most probable candidate, SiO_2 was measured by spectroscopic ellipsometry (SPORA, GESP-5). The results are shown in Fig. 6. The SiO_2 layer on the silicon surface irradiated by x-ray photons is clearly thicker than that on the unirradiated surface. The cleaned silicon surface is terminated by hydrogen atoms. X-ray photons are considered to break the H–Si bond, then O atoms or OH^- radicals adsorb to the dangling bonds. Finally, the thin crystal is bent because of the membrane stress leading to the shadow evolution.

These results indicate that the initial (wide) effective splitting area persists in a helium atmosphere. Although the oxidation is also blocked in vacuum, operation in vacuum probably leads to critical lattice vibration after the impact of XFEL pulses.[11] Further, the thermal conductivity of helium gas is 6 times greater than that of ambient air. This means a high thermal contact with the ultrathin silicon crystal can be accomplished without any metal contacts, which could possibly introduce mechanical stress to the crystal. Therefore, a helium atmosphere is considered to be the best operation condition for the applications of ultrathin crystals.

5. CONCLUSIONS

A new fabrication technique for ultrathin silicon crystals based on PCVM was developed. The high quality of the fabricated crystals was verified with topographic and high-resolution rocking curve measurements at SPring-8. As an application of the ultrathin crystal, a non-destructive arrival-time monitor system was constructed and installed at SACLA. A total of three sub-10-μm-thick Si(220) crystals were prepared and tested for a split-delay unit with a high throughput and a wide energy range. A SiO_2 layer was grown on a silicon surface under x-ray irradiation, which probably induced lattice bending because of the membrane stress. Oxidation could be prevented by operating the thin silicon crystals in a helium atmosphere. Further, the proposed PCVM technique can be applied for other materials such as diamond. Potential applications of the fabrication technique will realize the development of future x-ray sources such as an XFEL oscillator[17] and a wide range of scientific findings at XFEL facilities.

ACKNOWLEGEMENTS

The authors thank the staff of SACLA/SPring-8 for their continuous support. This study was partially supported by the Proposal Program of SACLA Experimental Instruments of RIKEN, Grant-in-Aid for JSPS Fellows from Japan Society for the Promotion of Science, and the Global COE Program from the Ministry of Educatijon, Sports, Culture, Science and Technology, Japan.

REFERENCES

[1] Emma, P. *et al.*, "First lasing and operation of an ångstrom-wavelength free-electron laser," Nature Photon. **4**, 641–647 (2010).

[2] Ishikawa, T. *et al.*, "A compact X-ray free-electron laser emitting in the sub-ångström region," Nature Photon. **6**, 540–544 (2012).

[3] Young, L. *et al.*, "Femtosecond electronic response of atoms to ultra-intense X-rays," Nature (London) **466**, 56–61 (2010).

[4] Fukuzawa, H. *et al.*, "Deep Inner-Shell Multiphoton Ionization by Intense X-Ray Free-Electron Laser Pulses," Phys. Rev. Lett. **110**, 173005 (2013).

[5] Chapman, H. N. *et al.*, "Femtosecond X-ray protein nanocrystallography," Nature (London) **470**, 73–77 (2011).

[6] Seibert, M. M. *et al.*, "Single mimivirus particles intercepted and imaged with an X-ray laser," Nature (London) **470**, 78–81 (2011).

[7] Glover, T. E. *et al.*, "X-ray and optical wave mixing," Nature (London) **488**, 603–608 (2012).

[8] Bionta, M. R. *et al.*, "Spectral encoding of x-ray/optical relative delay," Opt. Express **19**, 21855–21865 (2011).

[9] Bushuev, V. A., "Diffraction of x-ray free-electron laser femtosecond pulses on single crystals in the Bragg and Laue geometry," J. Synchrotron Rad. **15**, 495–505 (2008).

[10] Zhu, D. *et al.*, "A single-shot transmissive spectrometer for hard x-ray free electron lasers," Appl. Phys. Lett. **101**, 034103 (2012).

[11] Feng, Y. *et al.*, "Experimental Measurements of Ultra-Thin Bragg Crystals for LCLS Beam-Sharing Operation," J. Phys.: Conf. Ser. **425**, 052002 (2013).

[12] Osaka, T. *et al.*, "A Bragg beam splitter for hard x-ray free-electron lasers," Opt. Express **21**, 2823–2831 (2013).

[13] Tamasaku, K. *et al.*, "SPring-8 RIKEN beamline III for coherent X-ray optics," Nucl. Instrum. Methods Phys. Res. A **467–468**, 686–689 (2001).

[14] Harmand, M. *et al.*, "Achieving few-femtosecond time-sorting at hard X-ray free-electron lasers," Nature Photon. **7**, 215–218 (2013).

[15] Sato, T. *et al.*, "Development of ultrafast pump and probe experimental system at SACLA," J. Phys.: Conf. Ser. **425**, 092009 (2013).

[16] Roseker, W. *et al.*, "Development of a hard X-ray delay line for X-ray photon correlation spectroscopy and jitter-free pump-probe experiments at X-ray free-electron laser sources," J. Synchrotron Rad. **18**, 481–491 (2011).

[17] Kim, K.-J., Shvyd'ko, Yu., and Reiche, S., "A Proposal for an X-Ray Free-Electron Laser Oscillator with an Energy-Recovery Linac," Phys. Rev. Lett. **100**, 244802 (2008).